

# CLASSIFICATION OF SATELLITE CLOUD IMAGERY BASED ON MULTI-FEATURE TEXTURE ANALYSIS AND NEURAL NETWORKS

*C.I. Christodoulou<sup>1</sup>, S.C. Michaelides<sup>2</sup>, C.S. Pattichis<sup>1</sup>, K. Kyriakou<sup>1</sup>*

<sup>1</sup> Department of Computer Science, University of Cyprus,  
Kallipoleos 75, P.O.Box 20537, 1678 Nicosia, Cyprus  
e-mail: {cschr2, pattichi}@ucy.ac.cy

<sup>2</sup> Meteorological Service, 1418 Nicosia, Cyprus  
e-mail: cssilas@ucy.ac.cy

## ABSTRACT

The aim of this work was to develop a system based on modular neural networks and multi-feature texture analysis that will facilitate the automated interpretation of cloud images. This will speed up the interpretation process and provide continuity in the application of satellite imagery for weather forecasting. A series of infrared satellite images from the Geostationary satellite METEOSAT7 were employed in this research. Nine different texture feature sets (a total of 55 features) were extracted from the segmented cloud images using the following algorithms: first order statistics, spatial gray level dependence matrices, gray level difference statistics, neighborhood gray tone difference matrix, statistical feature matrix, Laws texture energy measures, fractals, and Fourier power spectrum. The neural network SOFM classifier and the statistical KNN classifier were used for the classification of the cloud images. Furthermore, the classification results of the different feature sets were combined improving the classification yield to 91%.

## 1. INTRODUCTION

Geostationary satellites have long been established as excellent cloud observing platforms for various meteorological applications, primary of which is short range weather forecasting. Cloud patterns observed from such satellites are interpreted from expert meteorologists and are used in conjunction with several other weather forecasting tools in their day-to-day practice [1].

Clouds are customarily classified in three decks (etages): as Low, Medium or High, depending, among several other criteria, on the shape and distance of the cloud base from the ground. This kind of classification has been internationally agreed and used by meteorological services worldwide. The cloud identification, by using the

combined ground and satellite observations, is further complicated by the fact that the weather observers report cloud as seen from below, whereas, the satellite senses remotely the cloud from above. In order to avoid the confusion, which may arise because of this discrepancy, in this work, only areas on the satellite image with a single deck of cloud were analysed.

Because the interpretation of satellite images by individual weather forecasters implies a high level of personal estimation and subjectivity, artificial neural networks [2] have been employed in previous work, in order to establish an objective methodology for such an interpretation [1], [3], [4]. Neural networks use in image texture analysis and in cloud classification has also recently been shown [5].

The findings in this work suggest that neural networks and multi-feature, multi-classifier analysis of satellite imagery provide a standardised and efficient way for classifying cloud types that can be used as an operational tool in weather analysis.

In the current study, the modules of the automated system for cloud classification are the following:

- (i) Texture feature extraction,
- (ii) Classification using neural networks and statistical classifiers,
- (iii) Combining of the classification results.

The system should be able to classify cloud images into one of the following six cloud types: altocumulus-altostratus (ACAS), cumulonimbus (CB), cirrus-cirrostratus (CICS), cumulus-stratocumulus (CUSC), stratus (ST) and clear conditions (CLEAR). Some of these cloud types like CUSC, ACAS and CICS are group-types representing clouds usually observed together. It should be emphasised that the labelling of the different cases was done by agreed combined ground and satellite observations.

## 2. MATERIAL

The satellite images used in this work consist of the 0000, 0600, 1200 and 1800UTC images corresponding to the main synoptic observing times. The satellite images were contrasted to the actual observations reported at the earth's surface at the above times. These observations are plotted on the respective synoptic maps archived at the Meteorological Office Larnaka Airport in Cyprus. Using this standardized information from the human observers on the ground and the expertise of a meteorologist, cloud types were identified on the satellite images and classified manually accordingly.

From a total number of 98 satellite images, 366 samples, representing six cloud types, were manually classified by the expert meteorologist. The cloud region of interest was manually outlined and saved for feature extraction.

## 3. METHOD

In the feature extraction module multiple texture features were extracted from the manually classified samples in order to be used for classification. Texture contains important information, which is used by humans for the interpretation and the analysis of many types of images. Texture refers to the spatial interrelationships and arrangement of the basic elements of an image [6]. Visually, these spatial interrelationships and arrangements of the image pixels are seen as variations in the intensity patterns or gray tones. Therefore texture features have to be derived from the gray tones of the image. Although it is easy for humans to recognise texture, it is quite a difficult task to be defined, and subsequently to be interpreted by digital computers.

For the satellite images used in this study, nine different texture feature sets (a total of 55 features) were extracted using the following algorithms. The features were normalised before use.

(i) *First Order Statistics (FOS)* [7]

1) Mean value, 2) Median value, 3) Standard Deviation, 4) Skewness, 5) Kurtosis.

(ii) *Spatial Gray Level Dependence Matrices (SGLDM)* [8]

1) Angular second moment, 2) Contrast, 3) Correlation, 4) Sum of squares: variance, 5) Inverse difference moment, 6) Sum average, 7) Sum variance, 8) Sum entropy, 9) Entropy, 10) Difference variance, 11) Difference entropy, 12), 13) Information measures of correlation. For each feature the mean values and the range of values were computed, and were used as two different feature sets.

(iii) *Gray Level Difference Statistics (GLDS)* [9]

1) Contrast, 2) Angular second moment, 3) Entropy, 4) Mean.

(iv) *Neighborhood Gray Tone Difference Matrix (NGTDM)* [6]

1) Coarseness, 2) Contrast, 3) Business, 4) Complexity, 5) Strength.

(v) *Statistical Feature Matrix (SFM)* [10]

1) Coarseness, 2) Contrast, 3) Periodicity, 4) Roughness.

(vi) *Laws Texture Energy Measures (TEM)* [11], [12]

1) LL - texture energy from LL kernel, 2) EE - texture energy from EE kernel, 3) SS - texture energy from SS kernel, 4) LE - average texture energy from LE and EL kernels, 5) ES - average texture energy from ES and SE kernels, 6) LS - average texture energy from LS and SL kernels.

(vii) *Fractal Dimension Texture Analysis (FDTA)* [12],[13]  
 $H^{(k)}$  parameter (Hurst coefficient) for resolutions  $k=1, 2, 3$ .

(viii) *Fourier Power Spectrum (FPS)* [9]

1) Radial sum, 2) Angular sum.

Following the texture feature extraction, classification was implemented using: (i) the neural network self-organizing feature map (SOFM) classifier [14], and (ii) the statistical K-Nearest Neighbor (KNN) classifier.

The SOFM was chosen because it is an unsupervised learning algorithm where the input patterns are freely distributed over the output node matrix [14]. The weights are adapted without supervision in such a way, so that the density distribution of the input data is preserved and represented on the output nodes. This mapping of similar input patterns to output nodes, which are close to each other, represents a discretisation of the input space, allowing a visualisation of the distribution of the input data. Figure 1 illustrates the distribution of each class on a 12x12 SOFM using as input all the 55 features. The figure illustrates the high degree of overlap between some of the six different classes.

The SOFM was trained for 5000 epochs with the 366 cloud patterns, and each pattern was assigned to one of the 144 output nodes of a 12x12 matrix. Similar patterns were assigned to the same output node. The classification for each pattern was implemented based on the class label of the rest of the patterns assigned to the same node. So the test pattern was said to belong to the majority of the rest of the patterns assigned to the same node. Because in this work the number of patterns per class was unequal, a bias was created in favour of the classes with a large number of members. In order to alleviate the above bias, the number of counted patterns on the node for each class, was multiplied with a correction factor. The correction factor was computed as the total number of patterns, (i.e. 366) divided by the number of members of each class. Thus, classes with a smaller number of members were given a greater weight in the classification process.

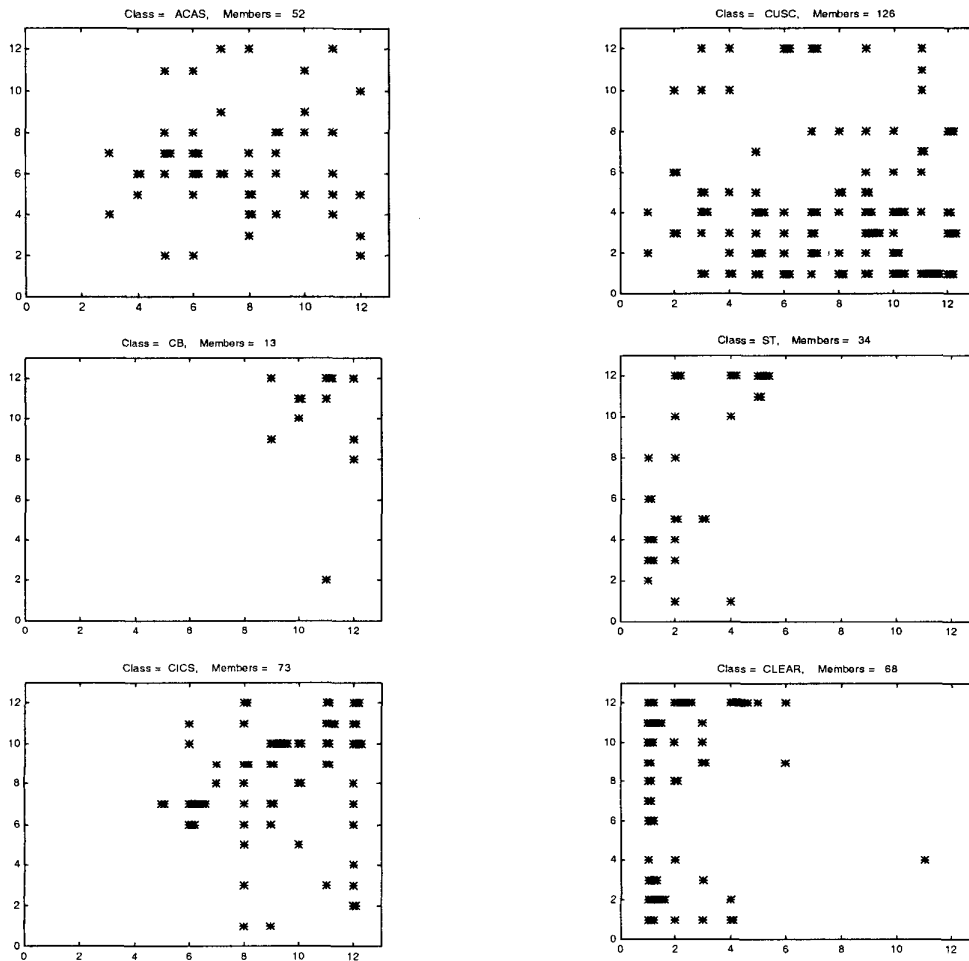


Figure 1: Distribution of the six cloud classes on a 12x12 SOFM matrix. The figure illustrates the overlap among the different classes.

The above procedure was repeated for each one of the 366 cloud patterns, using as input vector the nine different feature sets, i.e. nine different SOFM classifiers were trained and evaluated. Furthermore, modular neural networks [15] were used and the nine classification results were combined using the following combining techniques: (i) majority voting, and (ii) weighted averaging. In the majority voting the input pattern was assigned to the class of the majority of the nine classification results. In the weighted averaging case, the six class percentages of the number of patterns per class assigned to the output node, were summed up for the nine classifiers sets. The input pattern was assigned to the class with the greatest percentage value.

For comparison reasons, the statistical k-Nearest Neighbor (KNN) classifier was also implemented and used for cloud classification. In the KNN algorithm the  $k$  nearest neighbours of the test pattern were identified, based on their Euclidean distance. The test pattern was assigned to the class of majority of its  $k$  neighbours. The classification was implemented in a similar way to the SOFM classifier, using a correction factor and combining techniques. For the KNN classifier best results were obtained with  $k=3$ .

#### 4. RESULTS AND DISCUSSION

Table I tabulates the classification results for the SOFM and the KNN classifiers, for the nine texture feature sets, their average and when combined with majority voting and with weighted averaging. In the SOFM case, the results tabulated are the average of three different runs in order to obtain a more reliable output. Best results were obtained

with the SOFM classifier, with average for the nine feature sets 62.0%, whereas the KNN classifier yielded 50.2%. Best feature sets were for the SOFM the SGLDM (mean) with 67.1%, followed by the NGTDM with 64.8% and the SFM with 64.7%. For the KNN best feature sets were the SGLDM (mean) with 60.7%, followed by the FOS with 57.9% and the NGTDM with 54.1%. The classification yield of the SOFM modular system was significantly improved to 78.6% when combined with majority voting, and 91.2% when combined with weighted averaging. For the KNN system the yield was also improved to 61.2% with majority voting, and 64.2% with weighted averaging. The significant improvement of the classification yield in the combined results can be attributed to the relative large number of six classes. Due to that, misclassifications were distributed to a large number of classes and hence when combined easily compensated.

Table I Classification results of the cloud classification system.

	<i>Feature Set</i>	<i>SOFM</i>	<i>KNN</i>
1	FOS	64.0	57.9
2	SGLDM (mean)	67.1	60.7
3	SGLDM (range)	62.1	51.1
4	GLDS	64.7	53.0
5	NGTDM	64.8	54.1
6	SFM	64.7	52.2
7	TEM	63.3	51.9
8	FDTA	61.3	44.3
9	FPS	45.8	26.2
	<i>Average</i>	<i>62.0</i>	<i>50.2</i>
	<i>Combine with majority voting</i>	78.6	61.2
	<i>Combine with weighted averaging</i>	91.2	64.2

Table II Confusion matrix of the classification results among the six different classes.

<i>Cloud Class</i>	<i>Classified as</i>					
	<i>ACAS</i>	<i>CB</i>	<i>CICS</i>	<i>CUSC</i>	<i>ST</i>	<i>Clear</i>
<i>ACAS</i>	75.0	5.8	15.4	1.9	1.9	0.0
<i>CB</i>	0.0	92.3	7.7	0.0	0.0	0.0
<i>CICS</i>	12.3	13.7	71.2	2.7	0.0	0.0
<i>CUSC</i>	10.3	1.6	7.9	66.7	4.8	8.7
<i>ST</i>	0.0	0.0	0.0	0.0	88.2	11.8
<i>Clear</i>	2.9	0.0	1.5	7.3	27.9	60.3

Table II tabulates a confusion matrix of the classification results for the SOFM classifier, for the SGLDM (mean) feature set which yielded the best results. As seen from the table the ACAS clouds were most often misclassified as CICS and vice versa, whereas the same occurred with the

ST and the CLEAR classes. These results are in agreement with the pattern distribution displayed in Figure 1, and with the visual observation of the images.

In conclusion, the results in this work show that texture features can be successfully used for cloud classification and that a relatively good clustering of the different classes is provided. In addition, modular neural networks with multiple feature sets and combining techniques can significantly improve the classification yield of the system.

## 5. REFERENCES

- [1] Peak J.E., Tag P.M., "Towards automated Interpretation of Satellite Imagery for Navy Shipboard Applications", *Bulletin of the American Meteorological Society*, Vol.73, No.7, 995-1008, July 1992.
- [2] Haykin S., *Neural Networks – A comprehensive foundation*, Macmillan College Publishing Company, 1999.
- [3] Bankert R.L., "Cloud Classification of AVHRR Imagery in Maritime Regions Using a Probabilistic Neural Network", *Journal of Applied Meteorology*, Vol.33, No.8, 909-918, Aug. 1994.
- [4] Bankert R.L., Aha D.W., "Improvement to a Neural Network Cloud Classifier", *Journal of Applied Meteorology*, Vol.35, No.11, 2036-2039, Nov. 1996.
- [5] Tian B., Shaikh M., Azimi-Sadjadi M., Vonder Haar T., Reinke D., "A Study of Cloud Classification with Neural Networks Using Spectral and Textural Features", *IEEE Transactions on Neural Networks*, Vol. 10, No 1, Jan. 1999.
- [6] Amadasun M., King. R., "Textural Features Corresponding to Textural Properties", *IEEE Transactions on Systems, Man, and Cybernetics*, Vol. 19, No 5, Sept./Oct. 1989.
- [7] Press W.H., Flannery B.P., Teukolsky S.A., Vetterling W.T., *Numerical Recipes, The Art of Scientific Computing*, Cambridge University Press, Cambridge, 1987.
- [8] Haralick R.M., Shanmugam K., Dinstein I., "Texture Features for Image Classification", *IEEE Transactions on Systems, Man, and Cybernetics*, Vol.SMC-3, pp. 610-621, Nov. 1973.
- [9] Weszka J.S., Dyer C.R., Rosenfeld A., "A Comparative Study of Texture Measures for Terrain Classification", *IEEE Trans. on Systems, Man, & Cybernetics*, Vol. SMC-6, April 1976.
- [10] Wu Chung-Ming, Chen Yung-Chang, "Statistical Feature Matrix for Texture Analysis", *CVGIP: Graphical Models and Image Processing*, Vol. 54, No 5, pp. 407-419, Sept. 1992.
- [11] Laws K.I., "Rapid Texture Identification", *SPIE*, 1980, Vol. 238, pp. 376-380.
- [12] Wu Chung-Ming, Chen Yung-Chang, Hsieh Kai-Sheng, "Texture Features for Classification of Ultrasonic Liver Images", *IEEE Transactions on Medical Imaging*, Vol. 11, No 3, June 1992.
- [13] Mandelbrot B.B., *The Fractal Geometry of Nature*, San Francisco, CA, Freeman, 1982.
- [14] Kohonen T., "The Self-Organizing Map", *Proceedings of the IEEE*, Vol. 78, No. 9, pp. 1464-1480, Sept. 1990.
- [15] Perrone M.P., "Averaging/Modular Techniques for Neural Networks", *The Handbook of Brain Theory and Neural Networks*, ed. by M.A. Arbib, MIT Press, Cambridge, Massachusetts, pp. 126-129, 1995.